Numerical Simulation of Air Flow Field in High-Speed Aviation Tank

Sheng-Zhe Shi[1,2(✉)], Fan Wang[1], Zai-Bin Zuo[1], and Jun Jiao[1]

[1] AVIC Special Vehicle Research Institute, HuBei JingMen 448035, China
Shishengzhe05011232@126.com

[2] Key Aviation Scientific and Technological Laboratory of High Speed Hydrodynamic, HuBei JingMen 448035, China

Abstract. In order to quantify the increment of wind speed for high-speed trailer, this paper proposes to set sixteen measurement points of wind speed increment on it. Then, the experimental results are compared with those obtained by using the CFD method. It is shown in this paper that calculation results are 2% smaller than the ideal values obtained at different wind speed experimental points under the trailer, which leads to a wind speed increment steady region. Besides, the experimental and calculation results of wind speed increment are 8–10% smaller than the ideal values in this region, respectively. CFD shows feasibility and practicability in the analysis of air flow field for high-speed aviation tank. Surface crafts tend to be significantly affected by wind speed, such as seaplane, wing-in-ground effect ship, planning hull. Therefore, trailer front equipment can be used to mitigate the impact of wind speed on the test result.

Keywords: High speed aviation trailer · Air flow field · Experiment · Computational fluid dynamics (CFD)

1 Introduction

AS the basic component of hydrodynamic experiment conducted on seaplane, high-speed aviation tank enables the movement of seaplane model on the water. Trailer is powered by a motor fitted with high-precision speed control system, which ensures that the velocity error falls below 1% for the trailer. Trailer operation has an immediate effect on the precision of model movement speed and the accuracy of experimental results.

The high-speed hydrodynamic laboratory at Special vehicle research institute (605) is the only laboratory engaged in the study of hydrodynamics and experimental aviation science and technology. It is experimental speed highest (25 m/s) and the longest (510 m) towing tank in China. It focuses on the research of seaplane and amphibious aircraft, aircraft ditching experiment, the other surface ships and underwater device experiment. High-speed aviation tank is used to conduct hydrodynamic experiment and pneumatic experiment in close proximity to water[1]. All wind tunnel experiments require a satisfactory flow field of wind tunnel, which means that the flow parameters in time and space must be consistent[4, 5]. The ship travelling on the water surface at a low speed

is usually affected insignificantly by wind speed [6, 7]. The quality of air flow field is essential for the seaplane, wing-in-ground effect ship, planning hull and so on. In order to reduce the impact of wind speed increment under the trailer, some high-speed aviation tank put model in the lead of trailer in seaplane experiment in overseas (Fig. 1).

Fig. 1. Towing tank at the Russian hydrodynamic research institute

2   Air Flow Field Experiment in High Speed Aviation Tank

The air flow field experiments on high-speed aviation tank were conducted on 3–5 November 2009 at the high-speed hydrodynamic laboratory of Special Vehicle Research Institute (605). The measurement equipment included five hole pitot tubes and a micro pressure sensor complete with amplifier and temperature compensation. Five hole pitot tubes were demarcated in Wuhan university of technology fluid mechanics lab wind tunnel. The calibration of computer data acquisition software could be displayed in real time to record wind speed and its direction.

Two experimental sections are at before and after in the region of model (Fig. 2). There were 8 points in each experimental section, denoted as A1, B1, C1, D1, E1, A2, B2 and C2, respectively (Fig. 3). The stability value of trailer speeds is 3, 6, 9, 12, 14, 15, 16 and 18m/s, respectively. A coordinate system is established at the middle profile bottom of the trailer. The trailer travels in the positive direction of X axis, the left direction is in the positive direction of Y axis, and the up direction is in the positive direction of Z axis. The direction of air flow on the horizontal and vertical planes of each measurement point oscillates within the plus or minus 2 degrees. It is acceptable in the error range of air flow and installation. It is considered that there is no deflection to the measurement region for air flow (Table 1).

Fig. 2. Longitudinal position schematic diagram of air flow field measurement point
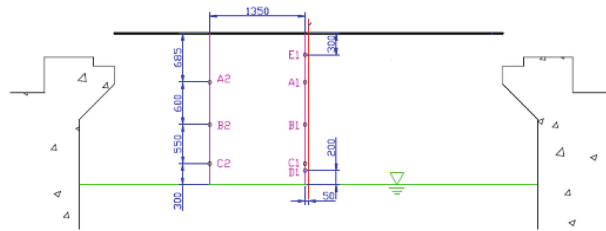

Fig. 3. Transverse position schematic diagram of air flow field measurement point

Table 1. Three-coordinate of air flow measurement points (unit: m)

Measurement point	X	Y	Z	Measurement point	X	Y	Z
1-A1	5.300	0.050	−0.685	2-A1	2.200	0.050	−0.685
1-A2	5.300	1.400	−0.685	2-A2	2.200	1.400	−0.685
1-B1	5.300	0.050	−1.285	2-B1	2.200	0.050	−1.285
1-B2	5.300	1.400	−1.285	2-B2	2.200	1.400	−1.285
1-C1	5.300	0.050	−1.835	2-C1	2.200	0.050	−1.835
1-C2	5.300	1.400	−1.835	2-C2	2.200	1.400	−1.835
1-D1	5.300	0.050	−1.935	2-D1	2.200	0.050	−1.935
1-E1	5.300	0.050	−0.300	2-E1	2.200	0.050	−0.300

3   Numerical Simulation of Air Flow Field in High Speed Aviation Tank

3.1   Basic Principles of Numerical Simulation

The core idea of numerical simulation is as follows: there are a series of variable value set of discrete points, instead of continuous physical field in the original time domain and space domain. The algebra equations of variable are established through certain principle and mode. Then, the algebra equations are solved to obtain the approximate

solution to variables. Numerical simulation mainly includes pre-treatment, solution and post-processing.

3.2 Mesh Model and Computational Domain of High Speed Aviation Tank

Compared with the actual situation, the computational domain of high-speed aviation tank is simplified in order to create mesh while reducing the calculation time. The breadth of computational domain is the breadth of workshop. The actual tank breath under the trailer is 6.5 m. In order to reduce the difficulty in dividing mesh and computing time, however, the tank breath under the trailer is set to the same level as workshop breadth. There is little impact made on the result (Table 2).

Table 2. Principal dimensions of mesh model and computational domain of high speed aviation tank (unit: m)

Project	Parameter	Project	Parameter
Length of trailer pedestal	8.7	Distance between trailer stern and outlet	10.0
Total length	9.2	Distance between trailer bottom and water surface	2.135
Breath of control room	2.2	Length of computational domain	30.0
Breath of trailer pedestal	7.0	Breath of computational domain	10.2
Height of trailer(include pedestal)	2.4	Height of computational domain	8.365
Height of trailer pedestal	0.4		

3.3 Divide Mesh

The computational domain range is an extremely wide one. The computing region is the air flow field under the trailer. By increasing model mesh under the trailer, the flow field accuracy of air flow under the trailer can be improved (Fig. 4).

4 Comparison Between Calculation Result and Experimental Result

Time model is stability, material model is air, and flow model is separation flow. The equation of state is ideal air, viscous model is turbulence, and Renault average turbulence model is K-Epsilon turbulence.

There are 16 measurement points calculated. The calculation results of wind speed are compared with the experimental results of wind speed at all points.

The comparisons performed between the ideal value, the calculation result and the experimental result of wind speed at all 16 points are showed from Figs. 5, 6, 7, 8, 9, 10, 11, 12, 13, 14, 15, 16, 17, 18, 19 and 20. It can be observed from these figures that:
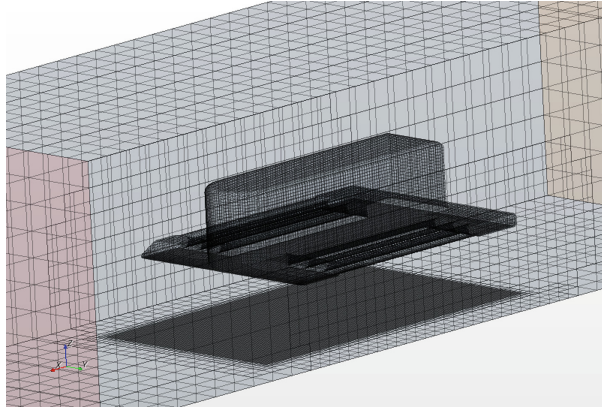
Fig. 4. Mesh model and computational domain of high-speed aviation tank
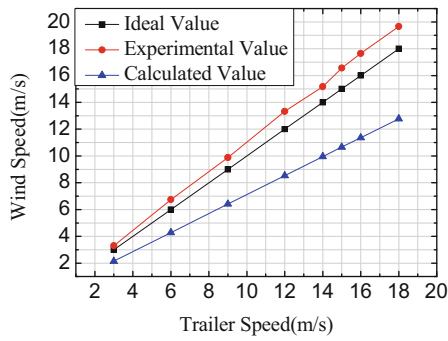

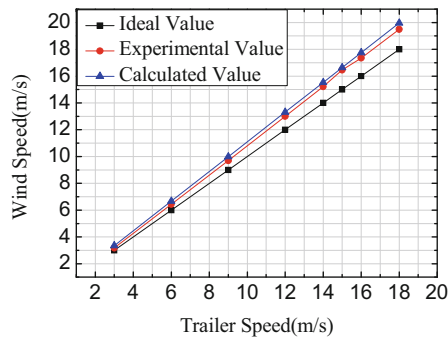**Fig. 5.** Comparison of ideal value, calculation result and experimental result of wind speed at 1-A1

Fig. 6. Comparison of ideal value, calculation result and experimental result of wind speed at 1-A2
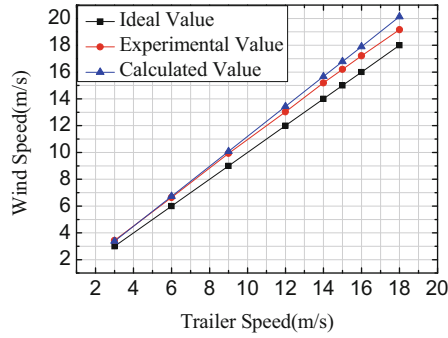
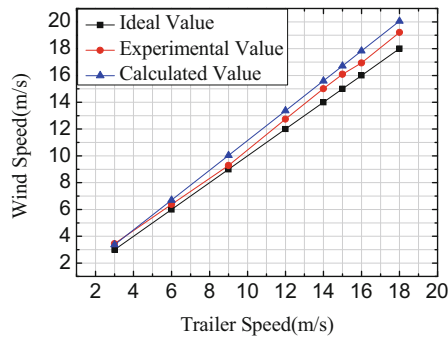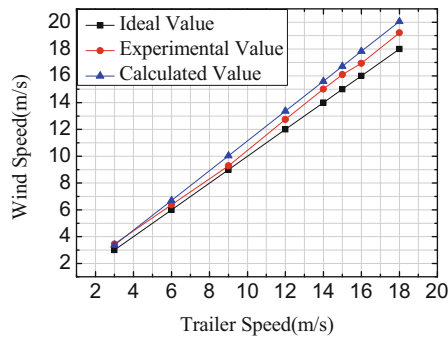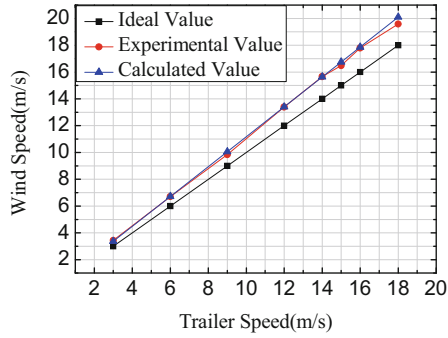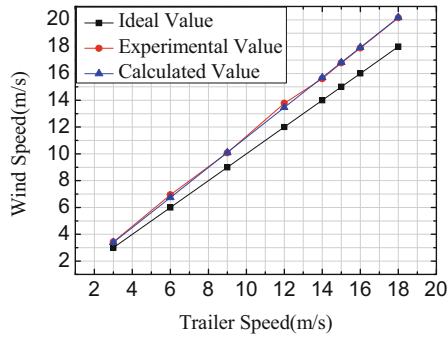**Fig. 7.** Comparison of ideal value, calculation result and experimental result of wind speed at 1-B1

Fig. 8. Comparison of ideal value, calculation result and experimental result of wind speed at 1-B2

Fig. 9. Comparison of ideal value, calculation result and experimental result of wind speed at 1-C1

(a) Except the measurement points 1-A1, 1-E1, 2-A1, 2-E1, the calculation results are 2% less than the ideal value at the other measurement points. Since the measurement points are closer to water surface, the errors are less significant. It is demonstrated

Fig. 10. Comparison of ideal value, calculation result and experimental result of wind speed at 1-C2

Fig. 11. Comparison of ideal value, calculation result and experimental result of wind speed at 1-D1
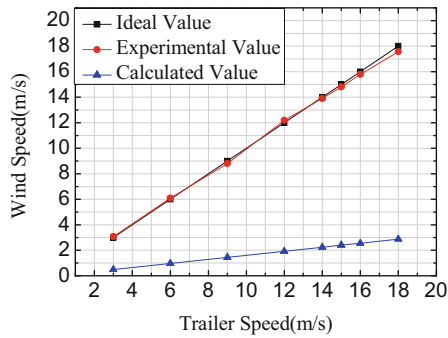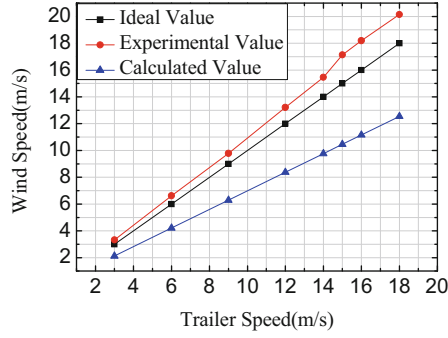

Fig. 12. Comparison of ideal value, calculation result and experimental result of wind speed at 1-E1

that CFD numerical simulation is suitable for analyzing the air flow field in high-speed aviation tank. The error of ideal value, calculation result and experimental result of wind speed at all measurement points makes no significant difference to

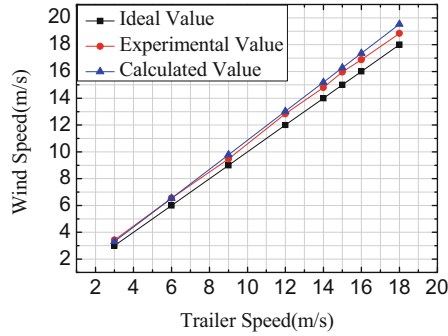**Fig. 13.** Comparison of ideal value, calculation result and experimental result of wind speed at 2-A1

Fig. 14. Comparison of ideal value, calculation result and experimental result of wind speed at 2-A2
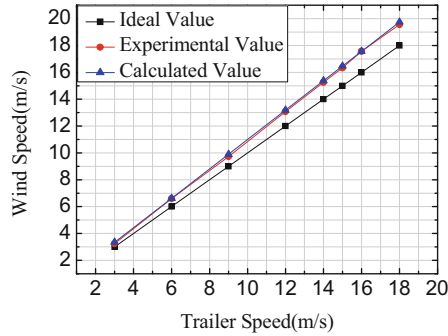

Fig. 15. Comparison of ideal value, calculation result and experimental result of wind speed at 2-B1

travel speed of the trailer. It shows that the increment of wind speed under the trailer is a natural result from the blocking effect.
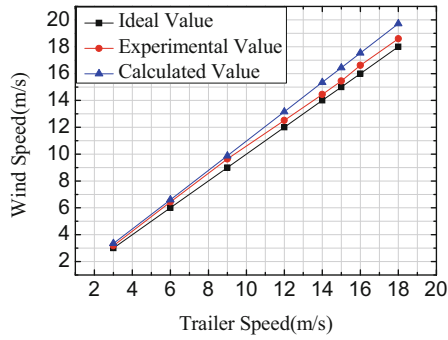
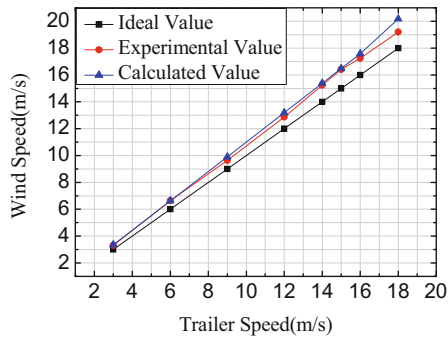**Fig. 16.** Comparison of ideal value, calculation result and experimental result of wind speed at 2-B2

Fig. 17. Comparison of ideal value, calculation result and experimental result of wind speed at 2-C1
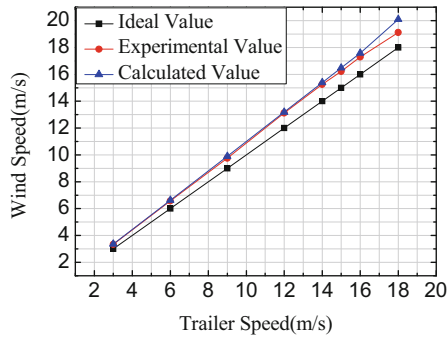

Fig. 18. Comparison of ideal value, calculation result and experimental result of wind speed at 2-C2

(b) As shown in Figs. 5, 7 and 9, the measurement point 1-A1 is closer to the trailer than the measurement points 1-B1 and 1-C1. Due to the effect of trailer boundary layer viscous, the calculation results of wind speed at the measurement points close
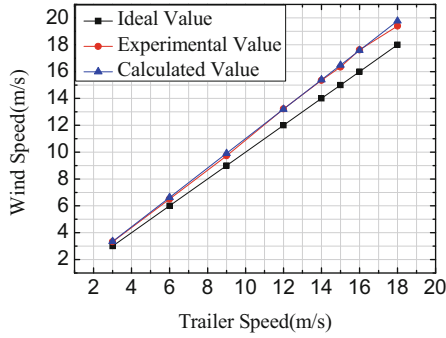
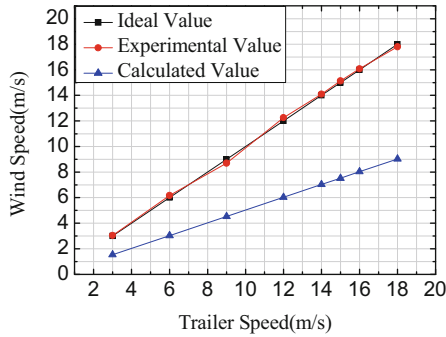**Fig. 19.** Comparison of ideal value, calculation result and experimental result of wind speed at 2-D1

Fig. 20. Comparison of ideal value, calculation result and experimental result of wind speed at 2-E1

to the trailer are smaller compared to those far from the trailer. In Fig. 12, it is more obvious that the calculation result of wind speed is smaller at the measurement point 1-E1. However, the difference isn't significant in the experiment, because the bottom of trailer isn't a plane in practice. In order to facilitate installation and observation, the bottom of the trailer is made open at about 0.8m breadth. When air flows through the opening, it will enter into the trailer, and wind speed wouldn't be sharply reduced. The bottom of the trailer is close flat at modelling, with no pressure inlet at the bottom of the trailer for air to flow inwards. It can cause the error of calculation and experimental results. In Fig. 12, the error of wind speed at the measurement point 1-E1 approaches 80%. As shown in Fig. 20, the error of wind speed at the measurement point 2-E1 is close to 50%. This is mainly because the mesh model of the trailer is different from the actual situation.

(c) In Figs. 7, 8 and 11, the measurement points 1-B1, 1-C1 and 1-D1 are far from the bottom of the trailer but close to the water surface. It is less significant that the measurement points are affected by the trailer boundary layer, but the blocking effect caused by the trailer persists. The calculation and experimental results are about 8–10% larger than the ideal value at the three measurement points, respectively. The

calculation result is almost identical to the experimental result. The error of three experimental results with each other is close to 2%, which shows that this height range is far from the bottom of trailer but close to the water surface. Differently, wind speed is stable at different positions of the range, which makes it usually the most important area for seaplane experiment.

(d) In Figs. 5, 7 and 9, the measurement points 1-A1, 1-B1, 1-C1 are in the front experimental section under the trailer. In Figs. 13, 15 and 17, the measurement points 2-A1, 2-B1, 2-C1 are in the after experimental section under the trailer. The corresponding calculation results and experimental results are comparable at the measurement points 1-A1, 1-B1, 1-C1 and measurement points 2-A1, 2-B1, 2-C1. The experimental results at the front point are about 2% larger than experimental results at the after point. It shows that wind speed increment is highly stable along the direction in which the trailer travels.

(e) In Figs. 5, 7 and 9, the measurement points 1-A1, 1-B1, 1-C1 are close to the middle longitudinal profile under the trailer. In Figs. 6, 8 and 10, the measurement point 1-A2, 1-B2, 1-C2 are far from the middle longitudinal profile under the trailer. The experimental error at the measurement point 1-A2 is less significant than the error at the measurement point 1-A1. This is possibly because the measurement point 1-A2 falls outside the region of breath of the control room and the impact of trailer boundary layer viscous is insignificant. This phenomenon persists at the measurement points 1-B1, 1-C1, 1-B2 and 1-C2. These measurement points are within the stable range of wind speed, and wind speed increment is stabilized at 8–10%.

The wind speed isolines and wind speed streamlines obtained in different sections when the trailer speed is 3 m/s, 9 m/s, or 16 m/s are showed from Figs. 21, 22, 23, 24, 25, 26, 27, 28 and 29, respectively. Through observation, it can be found out that:
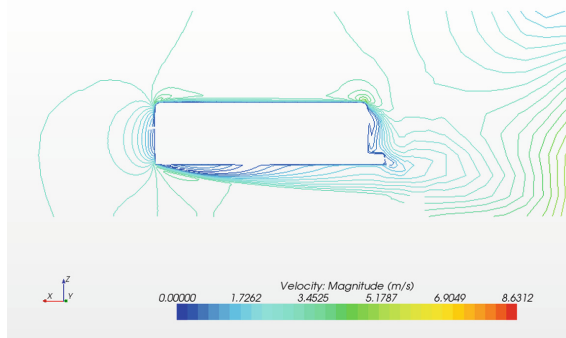

Fig. 21. Wind speed isoline in section Y = 0.05 m, when the trailer reaches a speed of 3 m/s

(f) In Figs. 21, 22, 24, 25, 27 and 28, the wind speed increment region shows no significant change with the speed at which the trailer travels. Wind speed isolines
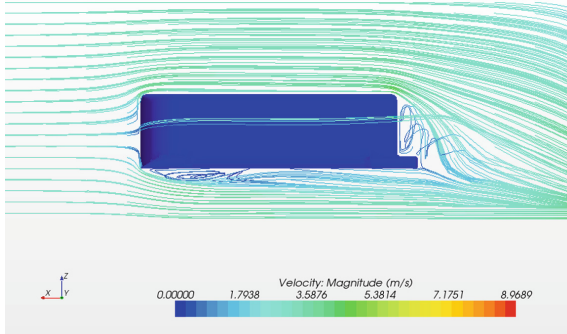
Fig. 22. Wind speed streamline in section Y = 0.05 m, when the trailer reaches a speed of 3 m/s
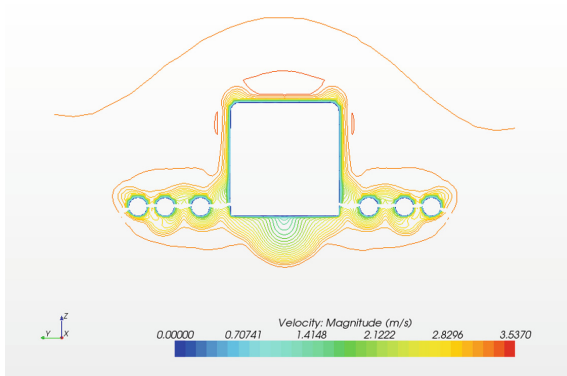

Fig. 23. Wind speed isoline in section X = 2.20 m, when the trailer reaches a speed of 3 m/s
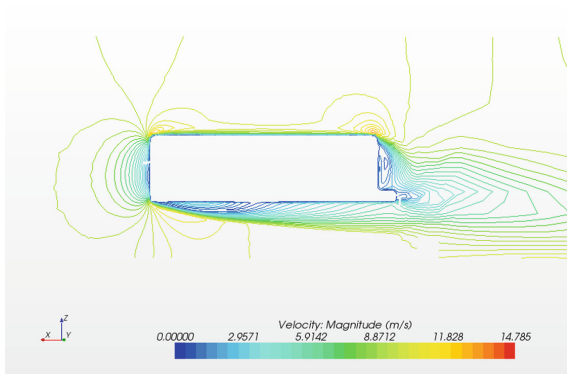

Fig. 24. Wind speed isoline in section Y = 0.05 m, when the trailer reaches a speed of 9 m/s
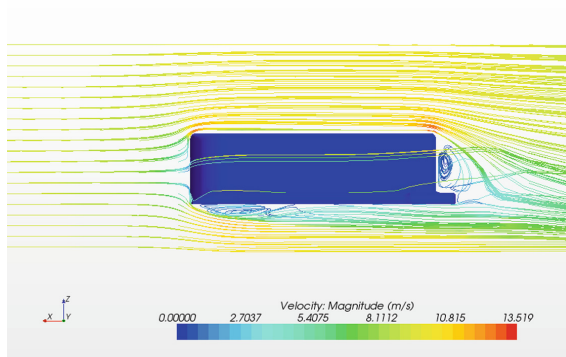
Fig. 25. Wind speed streamline in section Y = 0.05 m, when the trailer reaches a speed of 9 m/s
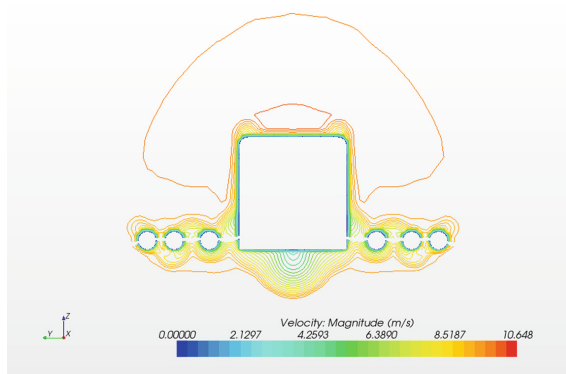

Fig. 26. Wind speed isoline in section X = 2.20 m, when the trailer reaches a speed of 9 m/s
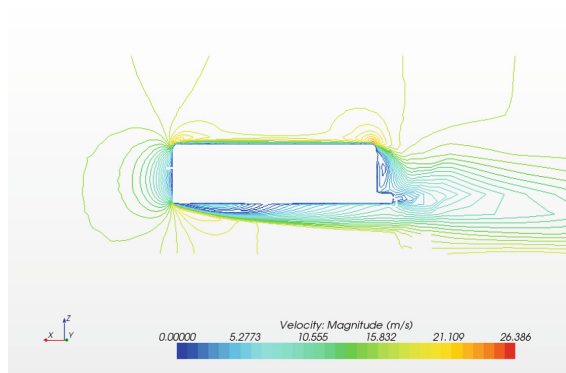

Fig. 27. Wind speed isoline in section Y = 0.05 m, when the trailer reaches a speed of 16 m/s
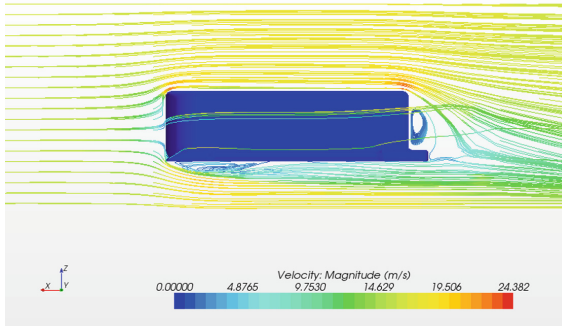
Fig. 28. Wind speed streamline in section Y = 0.05 m, when the trailer reaches a speed of 16 m/s
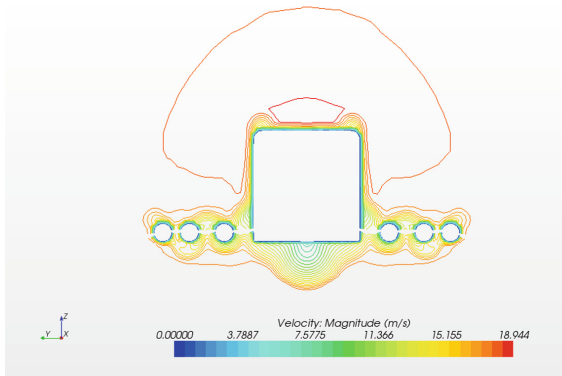

Fig. 29. Wind speed isoline in section X = 2.20 m, when the trailer reaches a speed of 16 m/s

and wind speed streamlines figure the result of comparison between the ideal value, the calculation result and experimental result of wind speed in a).

(g) Figures 21 and 22 show the effects of trailer boundary layer viscous. The region close to the bottom of the trailer is where the calculation result of wind speed is smaller. The range close to water surface but far from the bottom of the trailer is where wind speed is calculated to stabilize. Wind speed isolines and wind speed streamlines confirm the result of comparison between the ideal value, calculation result and experimental result of wind speed in (b) and (c).

(h) Figures 23, 26 and 27 show the effect of trailer boundary layer viscous in the region near the bottom of the trailer. There is a low wind speed range middle region formed under the trailer.

5   Conclusions

The numerical simulation of air flow field in high-speed aviation tank indicates that:

(1) Except 4 measurement points close to the bottom of the trailer, the calculation results are less than 2% of the ideal value at the other measurement points. The closer to water surface, the less significant the error. It is suggested that CFD numerical simulation is suitable for the analysis of air flow field in high-speed aviation tank.
(2) The errors between the ideal value, the calculation result and the experimental result of wind speed at all measurement points don't change significantly with the speed at which the trailer travels. It shows that the wind speed increment under the trailer is related to the blocking effect.
(3) Due to the effect of trailer boundary layer viscous, the calculation results of wind speed are smaller at a point close to the bottom of the trailer than at the point far from the bottom of the trailer. Besides, the calculation results of wind speed at a transverse position close to the middle longitudinal profile are smaller than at a transverse position far from the middle longitudinal profile.
(4) The experimental results are 2% smaller than the ideal value at different measurement points distant from the bottom of the trailer but close to water surface. This leads to a stable wind speed increment region. The experimental results and calculation results are 8–10% smaller than the ideal value in the region.
(5) Wind speed has a significant impact on surface crafts, such as seaplane, wing-in-ground effect ship and planning hull. Therefore, trailer front equipment can be built to reduce the impact of wind speed on the test result.

References

1. Chu, L.-T., Gu, B.: Model aerodynamic characteristics test in high speed aviation tank. In: Seaplane Symposium. Aviation Industrial Publishing, Beijing, pp. 349–357 (2011) (in Chinese)
2. Li, S.O.N.G., Rui, T.I.A.N., Zhan-Feng, L.I.U., Rui-Xing, W.A.N.G.: The research is based on the CFD for the speed uniformity on the exports section of low-speed wind tunnel. J. Inner Mongolia Agricult. Univ. **32**(2), 199–201 (2011). (in Chinese)
3. Xi-Fang, L.Y.U., Fan, L.I.U.: The design and establishment of air dynamic wind tunnel. J. Environ. Hygiene **3**(4), 356–360 (2013). (in Chinese)
4. Xun-Nian, W.A.N.G., Ming-Hong, Z.H.U., Xiao-Dong, G.O.N.G.: Current state and shortage of low-speed wind tunnel testing on large civil aircraft. Aeronaut. Manuf. Technol. **2**, 95–98 (2009). (in Chinese)
5. Kun, H.U., Zhi-Jun, Z.H.A.O., Ting-Wei, Q.I.A.N.: Experiments investigation of the flow field in a simple wind tunnel. Mech. Res. Appl. **118**(2), 74–75 (2012). (in Chinese)
6. Lu, C., Jiang, Z., Wang, T.: Influences of different airflow situations for ship airwake. Ship Sci. Technol. **31**(9), 38–42 (2009) (in Chinese)
7. Hong, W.H., Jiang, Z.-F., Wang, T.: Infulence on air-wake with different layout of ship superstructure. Chin. J. Ship Res. **4**(2), 54–68 (2009) (in Chinese)